

This item was submitted to Loughborough's Institutional Repository (<https://dspace.lboro.ac.uk/>) by the author and is made available under the following Creative Commons Licence conditions.



**CC creative commons**  
COMMONS DEED

**Attribution-NonCommercial-NoDerivs 2.5**

**You are free:**

- to copy, distribute, display, and perform the work

**Under the following conditions:**

**BY:** **Attribution.** You must attribute the work in the manner specified by the author or licensor.

**Noncommercial.** You may not use this work for commercial purposes.

**No Derivative Works.** You may not alter, transform, or build upon this work.

- For any reuse or distribution, you must make clear to others the license terms of this work.
- Any of these conditions can be waived if you get permission from the copyright holder.

**Your fair use and other rights are in no way affected by the above.**

This is a human-readable summary of the [Legal Code \(the full license\)](#).

[Disclaimer](#) 

For the full text of this licence, please go to:  
<http://creativecommons.org/licenses/by-nc-nd/2.5/>

## Expansion of the plasma stability range in radio-frequency atmospheric-pressure glow discharges

J. J. Shi and M. G. Kong<sup>a)</sup>

*Department of Electronic and Electrical Engineering, Loughborough University, Loughborough, Leicestershire LE11 3TU, United Kingdom*

(Received 10 June 2005; accepted 14 September 2005; published online 7 November 2005)

Reliable applications of atmospheric-pressure glow discharges (APGDs) depend critically on their plasma stability. A common technique of ensuring APGD stability is to keep their operation well within their stability range by decreasing their discharge current. However, this reduces the achievable densities of the reactive plasma species and, thereby, compromises the application efficiency. In this letter, the use of high excitation frequencies in radio-frequency APGD is shown to substantially expand their stability range. It is also demonstrated that high-frequency operation introduces an added benefit of higher electron energy and greater electron density, thus enabling more abundant reactive plasma species and improved application efficiency. © 2005 American Institute of Physics. [DOI: 10.1063/1.2128691]

Large-volume atmospheric-pressure glow discharges (APGDs) are at the focal point of current low-temperature plasma research because of their exciting scope for new science and their immense potential for widespread applications.<sup>1–3</sup> They are usually generated between two parallel electrodes and at an excitation frequency either in the kilohertz range (1–100 kHz)<sup>1,4,5</sup> or in the radio-frequency (rf) range (1–100 MHz).<sup>6–10</sup> Their electron mean-free path is typically in the region of a few submillimeters, thus making it difficult to maintain plasma stability when their volume is increased to cater to industrial applications. To prevent APGDs from evolving into arc plasmas, a common strategy is to keep their operation well within their stability range by decreasing the discharge current. However, this reduces the maximum achievable density of the reactive plasma species and compromises the plasma reactivity that is critical to the efficiency of their intended applications.<sup>1,2</sup> Therefore, a key issue for APGD science is to expand their stability range to larger discharge currents with the same or improved plasma reactivity.

In the case of rf APGD, an effective solution can be realized by controlling their current-voltage characteristics. Recent experimental and numerical studies have shown that there exist two different glow modes, namely the  $\alpha$ -mode and the  $\gamma$ -mode.<sup>7,11–13</sup> rf APGDs in the  $\gamma$ -mode are usually associated with high discharge current density and negative differential conductivity.<sup>7,11–13</sup> The latter property suggests that thermal runaway may occur even though the rf power fed into the plasma is capped. So the  $\gamma$ -mode is fundamentally unstable. On the other hand, rf APGDs in the  $\alpha$ -mode operate at a low current density, typically less than 50 mA/cm<sup>2</sup> in helium and at 13.56 MHz, and their differential conductivity is positive.<sup>12</sup> So, their stability can be secured by simply restricting the input rf power to below an appropriate level. Significantly, rf APGDs must evolve from the  $\alpha$ -mode into the  $\gamma$ -mode before they become unstable.<sup>7,11–13</sup> This suggests that rf APGDs can be kept stable when their operation is maintained within the  $\alpha$ -mode.

As the discharge current density increases following gas breakdown, rf APGDs evolve from the  $\alpha$ -mode to the  $\gamma$ -mode.<sup>11,12</sup> The two glow modes are separated from each other by a critical current density,  $J_{cr}$ . So, if the boundary between the  $\alpha$ - and  $\gamma$ -modes can be extended to a large  $J_{cr}$ , the parametric range of the  $\alpha$ -mode is expanded thus offering a greater scope to satisfy different application requirements. Also desirable is that a large  $J_{cr}$  allows for large current densities in the  $\alpha$ -mode and this is likely to lead to the production of more reactive plasma species without compromising APGD stability. Given that reactive plasma species are key enablers for many applications,<sup>1–4,6</sup> large discharge current density without the danger of the glow-to-arc transition is highly desirable for efficient applications. In this letter, we propose a technique for increasing  $J_{cr}$  using high excitation frequency, and establish its validity through a detailed numerical evaluation of the underlying discharge physics.

Our numerical study is based on a one-dimensional self-consistent continuum model for helium rf APGDs.<sup>11,12</sup> Since the objective of this study is to establish the principle of the proposed technique, pure helium is considered as the background gas and the effects of impurity gases<sup>14</sup> will be studied in a future note. Our model includes six plasma species, namely the electron  $e$ , helium ion  $\text{He}^+$ , excited helium atom  $\text{He}^*$ , dimer helium ion  $\text{He}_2^+$ , excited dimer atom  $\text{He}_2^*$ , and background helium atoms  $\text{He}$ . Relevant reactions and transport coefficients are identical to those used in literature.<sup>11–14</sup> Rates for reactions involving electrons are expressed in terms of the electron mean energy rather than the local electric field for an accurate description of the electrode sheath region.<sup>11,14</sup> The gas pressure is 760 Torr, the electrode gap size is 4 mm and the gas temperature is set at 300 K. The secondary electron emission coefficient is 0.03.

The discharge current density and applied voltage characteristics of rf APGDs are shown in Fig. 1 at 6.78 MHz, 13.56 MHz, and 27.12 MHz. Each curve starts with the point of the minimum discharge current density,  $J_{min}$ , obtained immediately after gas breakdown. After  $J_{min}$ , the applied voltage increases with the discharge current density in the  $\alpha$ -mode until a critical current density above which the discharge voltage decreases with the current density in the

<sup>a)</sup> Author to whom correspondence should be addressed; electronic mail: m.g.kong@lboro.ac.uk

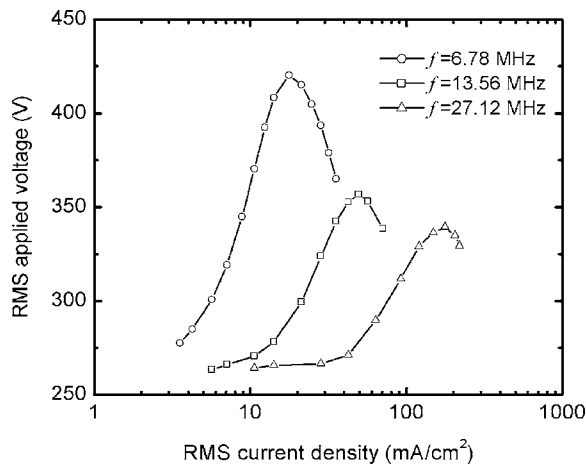


FIG. 1. Current-voltage characteristics of a helium rf APGD at three different frequencies.

$\gamma$ -mode. For the low frequency of 6.78 MHz, the critical current density is  $17.7 \text{ mA/cm}^2$  at an applied voltage of 420.2 V, and so the helium rf APGD is stable at current densities below  $17.7 \text{ mA/cm}^2$ . At 13.56 MHz and 27.12 MHz, the critical current density increases to  $49.5 \text{ mA/cm}^2$  and  $176.8 \text{ mA/cm}^2$ , respectively. So  $J_{cr}$  increases substantially by a factor of 10 ( $\approx 176.8/17.7$ ) over the four-fold frequency increment from 6.78 MHz to 27.12 MHz. The current ratio,  $J_{cr}/J_{min}$ , is found to increase also from 5.0 at 6.78 MHz, through 8.8 at 13.56 MHz, to 16.7 at 27.12 MHz, suggesting a much broadened parametric range of the  $\alpha$ -mode and hence a greater scope for APGD stability. In addition to the increased  $J_{cr}$  with increasing frequency, Fig. 1 also shows that the applied voltage at the critical current density decreases with increasing frequency. This pattern is very similar to an experimental observation made for helium rf APGDs with a 0.16 cm gap.<sup>6</sup>

The above observation may be understood from sheath characteristics. Following gas breakdown, a sheath region is formed near each electrode where the electric field is much higher than that in the bulk plasma region.<sup>7,8,11-14</sup> Sheath voltage is calculated in the same way as before<sup>11</sup> and its dependence on the discharge current is shown [Fig. 2(a)] to be very similar to the current-voltage characteristics in Fig. 1. Specifically, the point that separates positive differential conductivity from negative differential conductivity in the sheath region corresponds exactly to the conductivity separation point for the entire electrode gap, and as such it corresponds to the critical current density also. With an increasing current density in the  $\alpha$ -mode, the sheath thickness is shown [Fig. 2(b)] to shrink to a relatively constant value at each of the three frequencies, particularly so at 6.78 MHz. This near constant of the sheath thickness is about  $700 \mu\text{m}$ ,  $410 \mu\text{m}$ , and  $250 \mu\text{m}$  at 6.78 MHz, 13.56 MHz, and 27.12 MHz, respectively. When the discharge evolves into the  $\gamma$ -mode, the sheath thickness reduces more rapidly with increasing discharge current density, especially at the low frequency of 6.78 MHz.

Gas ionization in the  $\alpha$ -mode is known to be predominantly volumetric, spreading over both the sheath and the plasma bulk regions.<sup>11,12</sup> Electrons are accelerated largely by the oscillating rf field, and gain their kinetic energy accumulatively while moving from the electrodes toward the plasma bulk. Once their kinetic energy exceeds the ionization en-

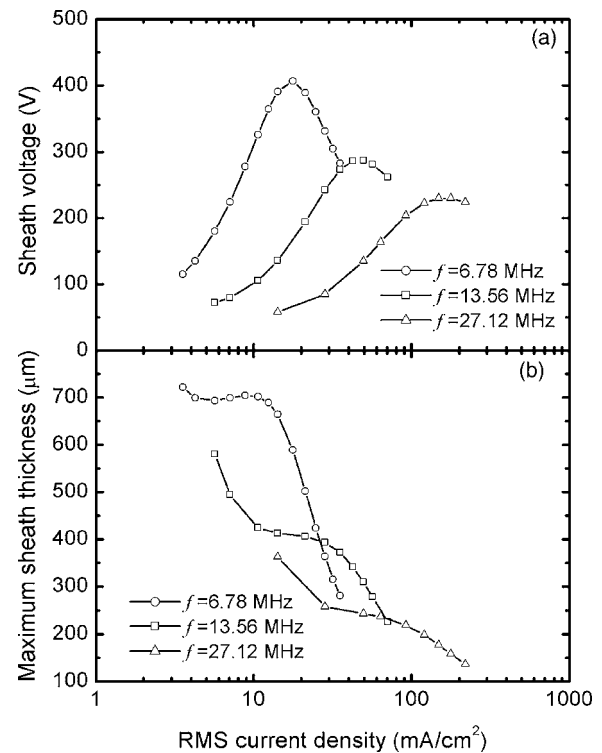


FIG. 2. Current density dependence of (a) the sheath voltage and (b) the maximum sheath thickness at three different frequencies.

ergy, new electron-ion pairs are created. Subsequently, the original electrons lose most of their kinetic energy and become ineffective for further ionization. This point marks the boundary of the sheath region with the plasma bulk region.<sup>11,12</sup> The sheath thickness depends on the spatial distance over which sufficient electrons are adequately accelerated to trigger an avalanche. At higher frequencies, the half-rf cycle is shorter and so electrons in the plasma bulk have less time to escape to the electrodes. The resulting reduction in electron loss makes it easier to achieve avalanche at higher frequencies. On the other hand since the sheath region alternatively swells into and shrinks from the plasma bulk during one rf cycle,<sup>12</sup> it captures some electrons that were previously in the plasma bulk. The reduced electron loss at higher frequencies enables more electrons to be captured by a swelling sheath, leading to more electrons being accelerated to exceed the ionization energy. In turn, this enables more new electron-ion pairs to be created over the same spatial distance. In other words, the availability of more sheath electrons at high frequencies leads to enhanced ionization thus making it easier to achieve avalanche. The combination of enhanced ionization and reduced electron loss is responsible for the narrow sheaths at high frequencies observed in Fig. 2(b). This also explains Fig. 2(a) where a smaller sheath voltage is sufficient to induce avalanche at higher frequencies.

Although the sheath voltage may be related qualitatively to the accumulated effect of electron acceleration toward the ionization energy, its value varies with the excitation frequency. As the frequency increases from 6.78 MHz to 27.12 MHz by a factor of 4, the sheath voltage is observed [Fig. 2(a)] to decrease from 406.9 V to 229.7 V by a factor of 1.8 and the sheath thickness is seen [Fig. 2(b)] to decrease from  $589.1 \mu\text{m}$  to  $158.0 \mu\text{m}$  by a factor of 3.7. It is known that the sheath region is depleted of electrons and so can be mod-

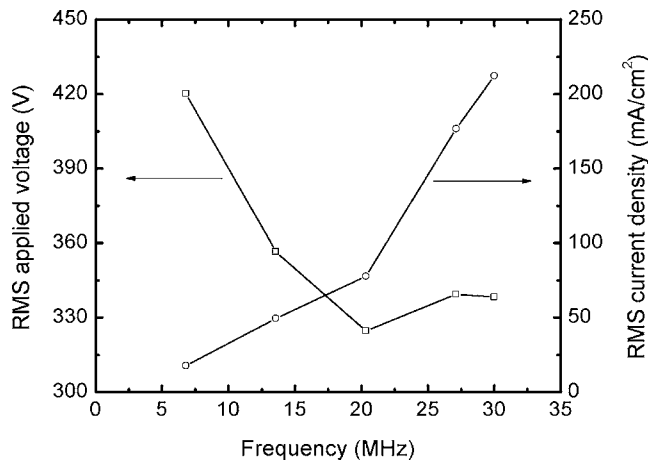


FIG. 3. Frequency dependence of the applied voltage and the discharge current density at the  $\alpha$ - $\gamma$ -transition point.

eled as a parallel-plate capacitor.<sup>7</sup> This suggests that the discharge current is carried over the sheath region predominantly through the displacement current. Therefore, the current density is  $J = (\epsilon_0/d_s)(dV_s/dt)$  with  $d_s$  and  $V_s$  being the sheath thickness and the sheath voltage, respectively.<sup>7</sup> As the frequency increases from 6.78 MHz to 27.12 MHz, a 3.7-fold reduction in sheath thickness, a 4-fold increase in  $d/dt$ , and a 1.8-fold reduction in the sheath voltage should combine to increase the current density by a factor of  $3.7 \times 4/1.8 = 8.2$ . This agrees well with the ten-fold increase in  $J_{cr}$  observed in Fig. 1. It is therefore clear that the range expansion of the  $\alpha$ -mode (Fig. 1) predominately benefits from the fact that high excitation frequency facilitates both efficient electron acceleration and large displacement current, both in the sheath region.

Figure 3 shows the frequency dependence of the applied rf voltage at the transition point between the  $\alpha$ -mode and the  $\gamma$ -mode. This transition voltage decreases from 420.2 V at 6.78 MHz to 324.7 V at 20.34 MHz, a net reduction of 22.7%. Then, it increases to 338.3 V at 30 MHz by a much smaller amount of 4.2%, suggesting a two-phase dependence on frequency. Similarly, the frequency dependence of the current density is shown (Fig. 3) to have a two-phase pattern. From 6.78 MHz to 20.34 MHz, the current density increases linearly from 17.7 mA/cm<sup>2</sup> to 77.8 mA/cm<sup>2</sup>. When the frequency is raised further, the current density increases more rapidly to 212.1 mA/cm<sup>2</sup> at 30 MHz. From 6.78 MHz to 30 MHz, the current density increases 12 fold (=212.1/17.7). This is much greater than the rate of voltage reduction, suggesting more powerful APGDs at high frequencies.

A larger current density achieved at a high excitation frequency is useful only when it leads to greater plasma reactivity. Plasma reactivity is influenced critically by the amount of reactive plasma species, and the latter depends on electron energy and density that determine the level of dissociation of the feed gases into reactive plasma species. Figure 4 shows the maximum electron-mean energy and the maximum electron density at the  $\alpha$ - $\gamma$ -transition point. As the

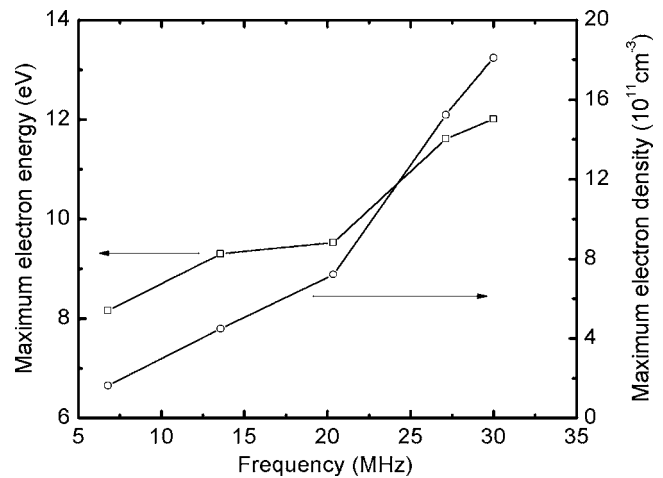


FIG. 4. Frequency dependence of the maximum electron mean energy and the maximum electron density at the  $\alpha$ - $\gamma$ -transition point.

excitation frequency increases from 6.78 MHz to 30 MHz, the maximum electron mean energy increases 1.5 times from 8.2 eV to 12.0 eV and the maximum electron density, 11 times from  $1.6 \times 10^{11} \text{ cm}^{-3}$  to  $18.1 \times 10^{11} \text{ cm}^{-3}$ . These suggest that high excitation frequency indeed leads to greater plasma reactivity.

In summary, the stability range of rf APGDs has been shown to expand considerably by increasing the plasma excitation frequency. A detailed study of sheath characteristics has demonstrated that sheath electrons are energized more efficiently at high frequencies. With the large displacement current at high excitation frequency, this leads to a sharp increase in the maximum permissible current density in the  $\alpha$ -mode. Finally, it has been established that high excitation frequency also increases electron energy and density, and so considerably improves plasma reactivity as well as application efficiency.

<sup>1</sup>J. R. Roth, *Industrial Plasma Engineering* (Institute of Physics Publishing, Philadelphia, PA, 1995), Vol. I.

<sup>2</sup>A. Schutze, J. Y. Jeong, S. E. Babayan, J. Park, G. S. Selwyn, and R. F. Hicks, *IEEE Trans. Plasma Sci.* **26**, 1685 (1998).

<sup>3</sup>M. Vleugels, G. Shama, X. Deng, E. Greenacre, T. Brocklehurst, and M. G. Kong, *IEEE Trans. Plasma Sci.* **33**, 824 (2005).

<sup>4</sup>F. Massine, A. Rabehi, P. Decomps, R. B. Gadri, P. Segur, and C. Mayoux, *J. Appl. Phys.* **83**, 2950 (1998).

<sup>5</sup>J. J. Shi and M. G. Kong, *Appl. Phys. Lett.* **86**, 091502 (2005).

<sup>6</sup>J. Park, I. Henins, H. W. Herrmann, and G. S. Selwyn, *J. Appl. Phys.* **89**, 20 (2001).

<sup>7</sup>J. J. Shi, X. T. Deng, R. Hall, J. D. Punnett, and M. G. Kong, *J. Appl. Phys.* **94**, 6303 (2003).

<sup>8</sup>Z. Yu, K. Hoshimiya, J. D. Williams, S. F. Polivinen, and G. J. Collons, *Appl. Phys. Lett.* **83**, 854 (2003).

<sup>9</sup>S. Wang, V. Schulz-von der Gathen, and H. F. Dobeles, *Appl. Phys. Lett.* **83**, 3272 (2003).

<sup>10</sup>E. Stoffels, A. J. Flikweert, W. W. Stoffels, and G. M. W. Kroesen, *Plasma Sources Sci. Technol.* **11**, 383 (2002).

<sup>11</sup>J. J. Shi and M. G. Kong, *J. Appl. Phys.* **97**, 023306 (2005).

<sup>12</sup>J. J. Shi and M. G. Kong, *IEEE Trans. Plasma Sci.* **33**, 624 (2005).

<sup>13</sup>X. Yang, M. Moravej, G. R. Nowling, S. E. Babayan, J. Panelon, J. P. Chang, and R. F. Hicks, *Plasma Sources Sci. Technol.* **14**, 314 (2005).

<sup>14</sup>X. Yuan and L. L. Raja, *Appl. Phys. Lett.* **81**, 814 (2002).